Hindawi
International Transactions on Electrical Energy Systems
Volume 2022, Article ID 7382210, 17 pages
https://doi.org/10.1155/2022/7382210

Research Article

Hierarchical Scheduling Control Method for Cascade Hydro-PV-Pumped Storage Generation System

Zhang Sun,[1,2] Jun Wang,[1] Sixiong Cheng,[3] Hong Luo,[1] Guosheng Zhang,[1] and Tao Huang[1]

[1]*School of Electrical Engineering and Electronic Information, Xihua University, Chengdu 610039, China*
[2]*School of Electrical Engineering, Southwest Jiaotong University, Chengdu 611756, China*
[3]*State Grid Neijiang Electric Power Company, Neijiang 641000, China*

Correspondence should be addressed to Jun Wang; wj.xhu@hotmail.com

Received 7 October 2021; Revised 29 April 2022; Accepted 13 May 2022; Published 30 June 2022

Academic Editor: François Vallée

High photovoltaic penetration in a power system has significantly challenged its safety and economic operation. To use the complementary characteristics of various renewable energy sources (RESs) fully, a novel hierarchical scheduling control (HSC) method is presented to accommodate the variability and uncertainty of a cascade hydro-PV-pumped storage (CH-PV-PS) generation system. Considering the optimization functions and execution requirements of the CH-PV-PS system, the HSC method is divided into two layers: the dynamic optimization layer and the static optimization layer. The static optimization layer focuses on the economy of the CH-PV-PS system, and the dynamic optimization layer focuses on the safety of the CH-PV-PS system. In the first layer, that is, the static optimization layer, the objectives of the day-ahead and hour-ahead schedules are established, and a heuristic algorithm is combined with a linear programming algorithm to optimize the energy allocation. Considering the uncertainty of the PV power output and hour-ahead load, a real-time schedule is established in the second layer; that is, in the second layer, the dynamic optimization layer, real-time scheduling and prediction of active output are established. Model predictive control methods are introduced to correct for prediction bias at different time scales in order to fully utilize the control capability of hydropower generation. A CH-PV-PS real-world system in Southwest China is chosen as a case study. In the three scenarios, where only PV fluctuations are considered, the simulation results reveal that, compared with the traditional open-loop optimized and hierarchical open-loop optimization methods, the HSC method reduces the average relative deviation of PV and increases the system economics. After a large amount of RESs are connected to the power grid, the HSC method provides a solution for improving the consumption of RESs.

1. Introduction

With the rapid development of renewable energy sources (RESs), such as photovoltaic (PV) and wind power, the RESs have been playing an increasingly important role in the energy system [1]. However, the randomness, intermittent characteristics, and strong volatility of PV seriously affect the security and reliability of the power system [2]. Thus, the operating PV power of the RESs, including hydropower or wind, has received great attention in recent years [3]. As a clean and renewable energy source, hydropower has a number of advantages, such as adjustable storage capacity, flexible starting and stopping, and fast response speed, which can be used to compensate for the intermittent output of PV [4].

Research on hydro-PV hybrid generation systems (HGSs) has mostly been focused on three aspects: optimal system size [5], operations management [6], and exploration of complementarity between hydropower and PV power. In terms of the exploration of complementarity of hydro-PV HGSs, the previous studies have investigated the complementarity between a single large-capacity power station and PV [7]. Based on the Longyangxia project, An et al. [8] presented complementary hydro-PV operation and proved that water and solar complementarity could improve the output quality of PV and reduce the peak load. Li and Qiu [9] proved that hydropower was the ideal compensation energy for PV and proposed an optimization model of hydro-PV generation. Liu et al. [10] proposed a three-layer

framework for large hydro-PV complementarity to formulate daily generation schedules. Zhang et al. [11] developed a high-order model for a hydro-PV power plant, which accurately quantified the effect of a water hammer on power quality. The complementary operation can effectively reduce PV waste, relieving the output of hydropower stations and improving the economic benefits of the system.

There are many hydropower plants combined with PV all over the world. For hydro-solar power complementary system, studies have been carried out in Longyangxia, China [12], northwestern Benin [13], northern Italy [14], and Rio Grande do Sul, Brazil [15]. Therefore, compared with a single large-capacity power station, it is essential to research the complementary operation of PV or other RESs with hydropower combined. Research has shown that battery energy storage or supercapacitors can augment the complementarity of hydro-PV HGSs. However, owing to the high investment and construction costs, low unit energy density, capacity degradation, and other problems, they are not ideal complementary combinations [16]. Compared with the other types of energy storage, the variable-speed pumped storage stations (VSPSSs) with full-size converters (FSCs) have the advantages of large capacity, mature technology, and rapid output adjustment [17]. The complementary characteristics between the spatial and temporal correlation characteristics of hydropower and PV and the output characteristics of the VSPSSs are suitable for compensating for rapid PV fluctuations. Thus, combining the cascade hydropower (CH) and PV with the VSPSSs to form a cascade hydro-PV-pumped storage (CH-PV-PS) generation system can provide complementary optimization of multiple RESs. Recently, a few studies have researched CH-PV-PS generation systems. Chen et al. [18] presented a fuzzy adaptive complete empirical mode decomposition method for PV fluctuation smoothing. Wu et al. [19] proposed a PV smoothing control method based on the wavelet packet CH-PV-PS complementary generation system. According to the coupling relationship of the CH-PV-PS reserve and generation, Jiang et al. [20] proposed a short-time scale offline reserve optimization. Li et al. [21] used seven-day hourly data to formulate a day-ahead optimization operation strategy for the PHS to maximize the economic benefits and similarity between the PHS generation curve and the load curve. Considering the uncertainty of PV, spot price, and load, Liu et al. [22] proposed a sizing model of the hydro-PV-pumped storage according to economics and complementary index. Huang et al. [23] proposed a day-ahead multiobjective stochastic optimal method for the CH-PV-PS system.

In the CH-PV-PS system, one of the greatest challenges is to consider the spatial-temporal coupling characteristics of the CH power station group and the uncertainty of inflow and PV involved in the system. Thus, solving the optimization and control problem is difficult under multitemporal and multispatial scales [24]. Most importantly are the variability of natural inflow and intermittency of PV introduce uncertainty to the decision-making process. In addition, meteorological factors have a large impact on the inflow and PV power generation, so the traditional optimal scheduling cannot meet the requirements of the CH-PV-PS system. Liu et al. [25] attenuated the effects of prediction errors by using renewable energy forecast data at different time scales. Huang et al. [26] established a convergent optimal control method for PV grid-connected network voltage in distribution networks based on multiple time scales to solve the voltage crossing limit and voltage fluctuation problems caused by PV grid-connected. Liu et al. [27]conducted global optimization and autonomous control strategies to coordinate the distributed power output in the active distribution network. In summary, the refinement of existing studies for time scales belongs to open-loop optimization, which can weaken the impact of uncertainty of new energy output to a certain extent, but the lack of feedback information on the actual operation status makes the deviation between the actual system operation and the dispatch expectation possible. Meanwhile, the existing literature is mostly devoted to the unilateral research on the scheduling or power coordination and control of complementary power generation systems, but there are few studies on multienergy complementation from the scheduling level combined with power coordination and control. And the existing multienergy complementation lacks studies on the complementary power generation with combined step: hydro and pumped storage and PV. These issues make complementary CH-PV-PS systems highly complex. However, the previous studies on the collaborative optimization of CH-PV-PS systems have been scarce [24]. Therefore, it is necessary to explore the collaborative optimization of CH-PV-PS systems from static optimization to dynamic execution and from extensive scheduling to accurate control.

Model predictive control (MPC) has three main features: predictive model, rolling optimization, and feedback correction. The MPC is an efficient alternative to deal with the uncertainty of the RES power generation under multiple time scales in multienergy complementary power generation systems [28].

To address the mentioned shortcomings, this paper studies the complementary operation of the CH-PV-PS system by considering the uncertainty of load and PV and the spatial-temporal coupling characteristics of the CH station group and PV. A hierarchical scheduling control (HSC) method is proposed to maximize the economic benefits, including generation efficiency and resource utilization, and to improve PV consumption and system stability. The HSC can be divided into two layers: static optimization layer and dynamic optimization layer. Moreover, considering the operation time requirements of dispatch control and the characteristics of various power generation units, the optimized execution schedule can be further divided into three time horizons: day-ahead, hour-ahead, and real time. In the day-ahead and hour-ahead optimizations, the static optimization layer is used to calculate unit start-stop schedules for the next day and the unit active output in the next hour. Using the MPC method and taking the output results of the static optimization layer as a reference, the dynamic optimization layer provides a rolling solution of the unit active output and decides whether to adjust the given prediction and actual operational requirements.

The main contributions of this paper can be summarized as follows:

(1) An HSC method for the complementary operation of the CH-PV-PS system is proposed. Compared with the traditional open-loop optimal scheduling, the PV generation capacity and comprehensive economic benefits of the system are improved while guaranteeing operational stability.

(2) Compared with the traditional open-loop optimized and hierarchical open-loop optimization methods, which only considers the improvement of the system scheduling ability due to the refinement time, the HSC method uses the rapid response ability of the pumped storage unit to respond to the rapid changes in photovoltaic output and load demand by introducing MPC. This enables the safety performance of the CH-PV-PS system to be improved.

The rest of the study is structured as follows. Section 2 introduces the CH-PV-PS generation system and presents the topology. Section 3 describes the HSC method. Section 4 introduces the optimal model and constraints. Section 5 demonstrates and discusses simulation results. Finally, Section 6 concludes the study.

2. CH-PV-PS System

The topology of the CH-PV-PS system in Xiaojin County, Sichuan Province, China, is presented in Figure 1, where it can be seen that this system consists of a centralized 50-MW PV station, 141-MW CHSs, and a 5-MW VSPSS. The output of each power generation unit in the CH-PV-PS system is supplied to a 220-kV AC bus. Then, the combined output of the CH-PV-PS system is sent to the utility grids. The energy management system (EMS) is the dispatch and control center, which sends reference power command to CHSs and VSPSS according to the predicted values of the load demand and PV output at different time scales.

3. HSC Framework

In the CH-PV-PS system, all generation units are clean and renewable. To improve the PV absorption and system stability, an HSC method for the CH-PV-PS system is proposed. The HSC framework is shown in Figure 2, where it can be seen that it mainly consists of a static optimization layer and a dynamic optimization layer.

The static optimization layer provides the day-ahead and hour-ahead schedules. It is mainly responsible for the optimal energy and economics allocation throughout the system, making the execution time more stable. In the static optimization layer, the day-ahead and hour-ahead schedules are used to solve the unit start-stop schedule in the $N{\cdot}\Delta T$ period and the unit's hour-ahead (ΔT period) operation schedule, respectively. The dynamic optimization layer, which is concerned with the real-time operation of the system, the scheduling problems caused by fluctuations in load and PV can be handled based on the load PV ultra-short-term forecast information, providing the output schedule of the unit in the $n{\cdot}\Delta t$ period. Scheduling control and unit operational requirements define the specific values of ΔT and Δt.

The day-ahead schedule is a start-stop schedule of the controllable generation unit in the $N{\cdot}\Delta T$ periods for guiding the unit operation during the day. The day-ahead schedule is a generation schedule issued by the dispatch system, considering the predicted PV and load, the dispatch control requirements, and the operational requirements of the system. The day-ahead schedule aims at maximizing the comprehensive economic benefits of a CH-PV-PS system.

The hour-ahead schedule is an active power output schedule of every controllable power generation unit in the ΔT period that issues the control command at the first time step. According to the hour-ahead forecast of the PV and load, the hour-ahead schedule can be used to correct the day-ahead schedule. In this way, not only the influence of uncertain factors is reduced, but also adjusting the real-time schedule directly based on the day-ahead schedule, which may cause large adjustments and bring adverse effects, is avoided.

The real-time schedule aims at adjusting forecast errors and ensuring system security. It uses the forecast information on the load and PV in an ultra-short-term scale and the output of the hour-ahead schedule as a reference to obtain an active output schedule value of the controllable generation unit in $n{\cdot}\Delta t$ period and delivers the result of the first time step. To realize accurate control of the controllable generation units in the system, the MPC method is introduced to realize a closed-loop control, and a detailed description is given in Section 4.2.

4. Mathematical Formulation

4.1. Static Optimization Layer

4.1.1. Day-Ahead Schedule. According to the generation schedule of a grid dispatch system, the objective function of the day-ahead schedule aims at maximizing the comprehensive economic benefits of a CH-PV-PS system. The dispatch control and operational requirements of the system are considered. The particle swarm optimization (PSO) and mixed-integer linear programming (MILP) are combined to solve the start-stop and output schedules of the controllable generation units in the $N{\cdot}\Delta T$ periods. In the modeling process, the fluctuating PV output is assumed to be perfectly consumed.

(1) Objective Function. The objective function is expressed as follows:

$$\begin{aligned} \max f^d &= \sum_{T=1}^{N} \left(C_T \left(U_T^T P_T^d + P_{s,T} \right) - C_{qT} P_{wT} - C_{sT} \left(U_T - D_T \right) \right), \\ P_T^d &= \left[P_{ij,T}, P_{f,T}, P_{p,T} \right], \\ P_{w,T} &= \left| P_{L,T} - P_T^d \right|. \end{aligned} \tag{1}$$

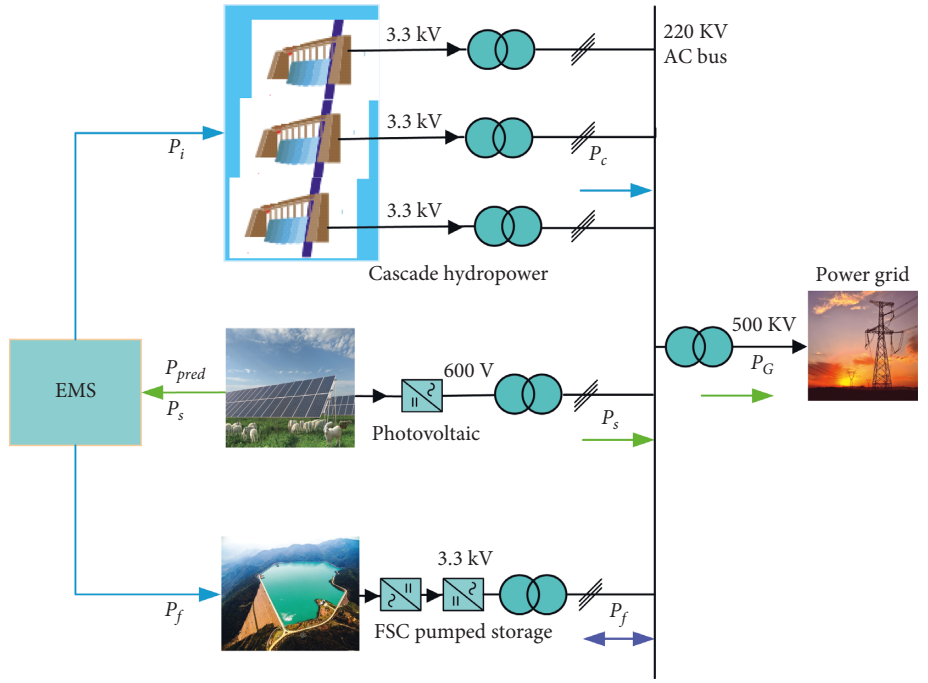

Figure 1: Topology of the CH-PV-PS system.

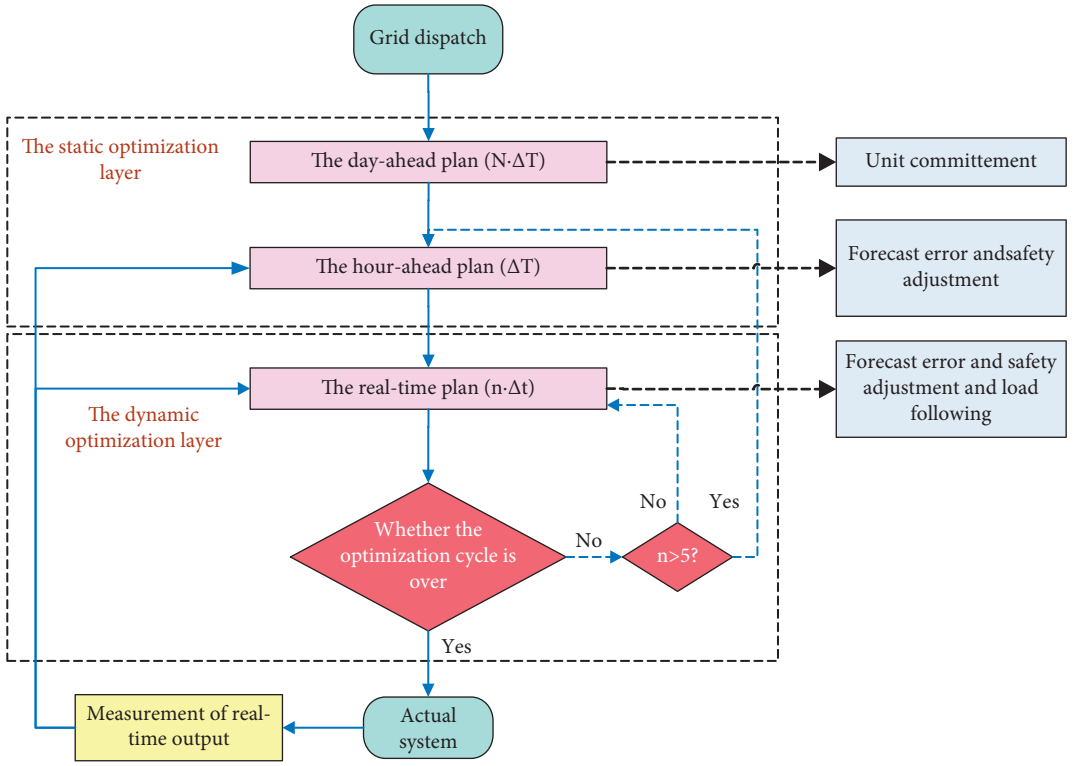

Figure 2: HSC framework for a CH-PV-PS system.

(2) Constraints. The day-ahead schedule considers multiple constraints, such as full consumption of the predicted PV generation, the scheduling control requirements of the CH-PV-PS system, and the operational constraints of CHSs. The constraints are defined as follows:

Reservoir balance constraint:

$$V_{i,T+1} = V_{i,T} + \left(I_{i,T} - Q_{i,T} - d_{i,T}\right) \times \Delta T. \tag{2}$$

Power balance constraint:

$$P_{L,T} = \mathbf{P}_T^d + P_{w,T}. \tag{3}$$

Generation inflow constraint:

$$Q_{i,\min} \le Q_i \le Q_{i,\max}. \tag{4}$$

Reservoir capacity constraint:

$$V_{i,\min} \le V_i \le V_{i,\max}. \tag{5}$$

Hydraulic head constraint:

$$H_{i,\min} \le H_i \le H_{i,\max}. \tag{6}$$

Output range constraint:

$$\mathbf{U}_T \mathbf{P}_{\min} \le \mathbf{P}_T^d \le \mathbf{U}_T \mathbf{P}_{\max}. \tag{7}$$

Vibration zone constraint:

$$\left(P_{ij,T} - P_{ij,T}^{up}\right)\left(P_{ij,T} - \underline{P_{ij,T}^{do}}\right) > 0. \tag{8}$$

Start and stop time constraints:

$$\begin{cases} U_{ij,T} - \sum_{T=T+1}^{T+T_{ijon}-1} D_{ij,T} \le 1, \\ D_{ij,T} - \sum_{T=T+1}^{T+T_{ijoff}-1} U_{ij,T} \le 1. \end{cases} \tag{9}$$

Ramp rate constraint:

$$\left|\mathbf{P}_{T+1} - \mathbf{P}_T\right| < \Delta \mathbf{P}^{\text{up}} \tag{10}$$

4.1.2. Hour-Ahead Schedule. Based on the hour-ahead forecasts of the PV and load, the hour-ahead schedule is used to correct the day-ahead schedule. Using the previous day-ahead schedule as a reference, the unit start-stop schedule considers multiple constraints, such as safety performance indicators. The objective function of the hour-ahead schedule aims at maximizing the comprehensive economic benefits. Hence, the hour-ahead scheduling specifies the active power output schedule of each controllable power generation unit in the ΔT period and outputs the first time step of the obtained schedule as a control command. The objective function is defined as

$$\max f^H = \sum_{t=T}^{T+\Delta T} \left(C_t\left(\mathbf{P}_t^H\right) - C_{qt} P_{wt}\right), \tag{11}$$

where

$$\mathbf{P}_t^H = \left[P_{ij,t}, P_{s,t}, P_{f,t}, P_{p,t}\right]. \tag{12}$$

Except for the constraints of the unit start and stop time defined by equation (9), the constraint conditions of the hour-ahead schedule are the same as those of the day-ahead schedule.

4.2. Dynamic Optimization Layer. The goal of dynamic optimization is to adjust the forecast error and ensure system security. Dynamic optimization uses the result of the static optimization layer and combines them with real-time forecast information on the load and PV and safe operational constraints to form a closed-loop control structure based on feedback correction. It specifies the active output schedule of the controllable generation unit in the period $n{\cdot}\Delta t$ and delivers the results for the first time step.

4.2.1. Objective Function. Taking the hour-ahead schedule result as a reference solution, the current output of each power generation unit of the CH-PV-PS generation system as an optimized initial value, and the active power output adjustment of the controllable generation unit in the system as a goal, the objective function can be established as follows:

$$\begin{aligned} \min f^m &= \sum_{\Delta t=1}^{n} \left(\mathbf{P}\left(t+\Delta t|t\right) - \mathbf{P}_r\left(t+\Delta t\right)\right)^2 \\ &= \sum_{\Delta t=1}^{n} \left(\mathbf{P}_0\left(t\right) + \sum_{k=1}^{\Delta t} \Delta \mathbf{p}\left(t+k|t\right) - \mathbf{P}_r\left(t+\Delta t\right)\right)^2. \end{aligned} \tag{13}$$

where

$$\begin{aligned} \mathbf{P}\left(t+\Delta t|t\right) &= \left[P_{ij}\left(t+\Delta t|t\right), P_f\left(t+\Delta t|t\right), P_p\left(t+\Delta t|t\right)\right], \\ \mathbf{P}_0\left(t\right) &= \left[P_{ij}\left(t\right), P_f\left(t\right), P_p\left(t\right)\right], \\ \mathbf{P}_r\left(t+\Delta t\right) &= \left[P_{ij}\left(t+\Delta t\right), P_s\left(t+\Delta t\right), P_f\left(t+\Delta t\right),\right. \\ &\qquad \left. P_p\left(t+\Delta t\right), \Delta P_s\left(t+\Delta t|t\right), \Delta P_L\left(t+\Delta t|t\right)\right]. \end{aligned} \tag{14}$$

The constraints of the real-time schedule mainly include power generation operational constraints and reserve safety margins. The interior point method is used to adjust the sequence of active power outputs for n future periods. The effect of the relationship between CHSs is not considered at this time scale. The constraints are defined as follows:

Output range constraint:

$$\mathbf{P}_{\min} \le \mathbf{P}_0\left(t\right) + \sum_{k=1}^{\Delta t} \Delta \mathbf{p}\left(t+k|t\right) \le \mathbf{P}_{\max}. \tag{15}$$

Ramp rate constraint:

$$\left|\mathbf{P}_{t+1} - \mathbf{P}_t\right| < \Delta \mathbf{P}^{m,\text{up}}. \tag{16}$$

Action dead zone constraint:

$$\left|\frac{\mathbf{P}_t - \mathbf{P}_{t+1}}{\mathbf{P}_t}\right| > \boldsymbol{\gamma}. \tag{17}$$

Vibration zone constraint:

$$\left(P_{ij,t} - P_{ij,t}^{\text{up}}\right)\left(P_{ij,t} - \underline{P_{ij,t}^{\text{do}}}\right) > 0. \tag{18}$$

Water release constraint:

$$Q_{i,\min} \le Q_{i,k} \le Q_{i,\max}. \tag{19}$$

4.2.2. Predictive Model. The prediction model predicts the future output based on the historical and future information on an object. The current measurement value of the system is used as an initial value, and the active power output adjustment sequence defined in Section 4.2.1 is used as an input prediction. Then, the active power output of a controllable power generation unit in the future period can be predicted. The prediction model is defined as follows:

$$\mathbf{P}(t+\Delta t|t) = \mathbf{p}_0(t) + \sum_{k=1}^{\Delta t} \Delta\mathbf{p}(t+k|t) \quad (\Delta t = 1, 2 \ldots n). \tag{20}$$

4.2.3. Feedback Correction. In actual systems, there exist errors between the forecasted PV and load values and the actual output, which may cause a mismatch between the schedule and actual response. Furthermore, it may make the system exceeding the safe operational constraints. Based on the MPC method, this study introduces the feedback correction link. To make the scheduling control results agree better with the actual output, the current active power output of the system is used as an initial value of the new time step of rolling optimization, which can effectively suppress the variability of the PV power output. The feedback correction is defined as follows:

$$\mathbf{p}_0(t+1) = \mathbf{p}_{\text{real}}(t+1). \tag{21}$$

To ensure that the deviation is within the allowable range, if the deviation exceeds a certain limit, it is necessary to adjust or reconstruct the load optimization distribution schedule of the real-time schedule or the hour-ahead schedule.

The real-time schedule is an adjusted schedule obtained when the deviation between scheduled output and actual output exceeds the predefined limit. The hour-ahead schedule is corrected when the results of the real-time schedule do not meet the requirements for a certain number of times, indicating the fact that the schedule cannot deal with the impact of uncertain factors in the system, so the load optimization distribution schedule needs to be reconstructed.

The dynamic optimization process is shown in Figure 3, and the specific steps are as follows:

(1) Use the PV and load rolling forecast model of the CH-PV-PS system to obtain the forecast information for the next optimization period and consider it an optimization input variable; use the current output of each controllable generation unit of the system as an initial optimization value.

(2) Use equation (20) as the active output prediction model of the controllable generation unit of the system and the active output adjustment as the controlled variable.

(3) Take the optimal output adjustment as a goal; calculate the active output adjustment for the next n periods by equation (13), which can be expressed as follows:

$$[\Delta\mathbf{p}(t+1|t), \Delta\mathbf{p}(t+2|t), \ldots \Delta\mathbf{p}(t+n|t)]. \tag{22}$$

(4) Obtain the active output forecast result at the first moment by

$$\mathbf{P}(t+1|t) = \mathbf{p}_0(t) + \Delta\mathbf{p}(t+1|t). \tag{23}$$

When the predicted output deviation is within the allowable range, do not adjust the output schedule. Take the actual output value of the system at $(t+1)$ time as an initial value of the new iteration of rolling optimization; namely, $p_0(t+1) = P_{\text{real}}(t+1)$. Then, perform the next iteration of optimization. If the predicted output deviation exceeds the limit range, $p_0(t+j) = P_{\text{real}}(t+j)$, reoptimize the output schedule. Similarly, when the active output schedule does not meet the requirements for a certain number of times during the optimization period, return to the hour-ahead schedule to restructure the generation schedule.

5. Case Study

To verify the effectiveness of the proposed HSC method, the CH-PV-PS system in Southwest China was used as a case study. The corresponding parameters of all power stations of the analyzed system are presented in Table 1. The comparison of the forecasted PV and load obtained by mathematical fitting from the operating data of the real system from 2017 to 2020 and the real output data is shown in Figure 4. The PV and load forecasting data are given by the researchers from our research group.

Considering the characteristics of each generation unit and the operation scheduling control requirements of the analyzed CH-PV-PS system, the day-ahead optimization scheduling period was set to 24 h, and the time resolution was set to 1 h. The optimal scheduling period of the hour-ahead schedule was 1 h, and the time resolution was 15 min. The optimal scheduling control period of the real-time schedule was 15 min, and the time resolution was 5 min. To verify the robustness of the proposed HSC method, sunny, cloudy, and rainy days were simulated. To simplify the analysis, the load data and the initial data, including the storage capacity and water head of the power station, were consistent in the three scenarios.

5.1. Simulation of PV Generation System on Sunny Days. According to the defined constraints, such as those of the forecast data and dispatch control requirements, the start and stop conditions of the power station units were obtained by the day-ahead schedule, and they are shown in Table 2. Unit 3 of all the power stations was shut down from 13:00 to 17:00 because the PV power generation was large during the day. During the high-output period, the shutdown of hydropower generating units could ensure the consumption of PV power generation and avoid unnecessary water abandonment, and the water stored in this period could be used for hydropower generation when the PV power generation

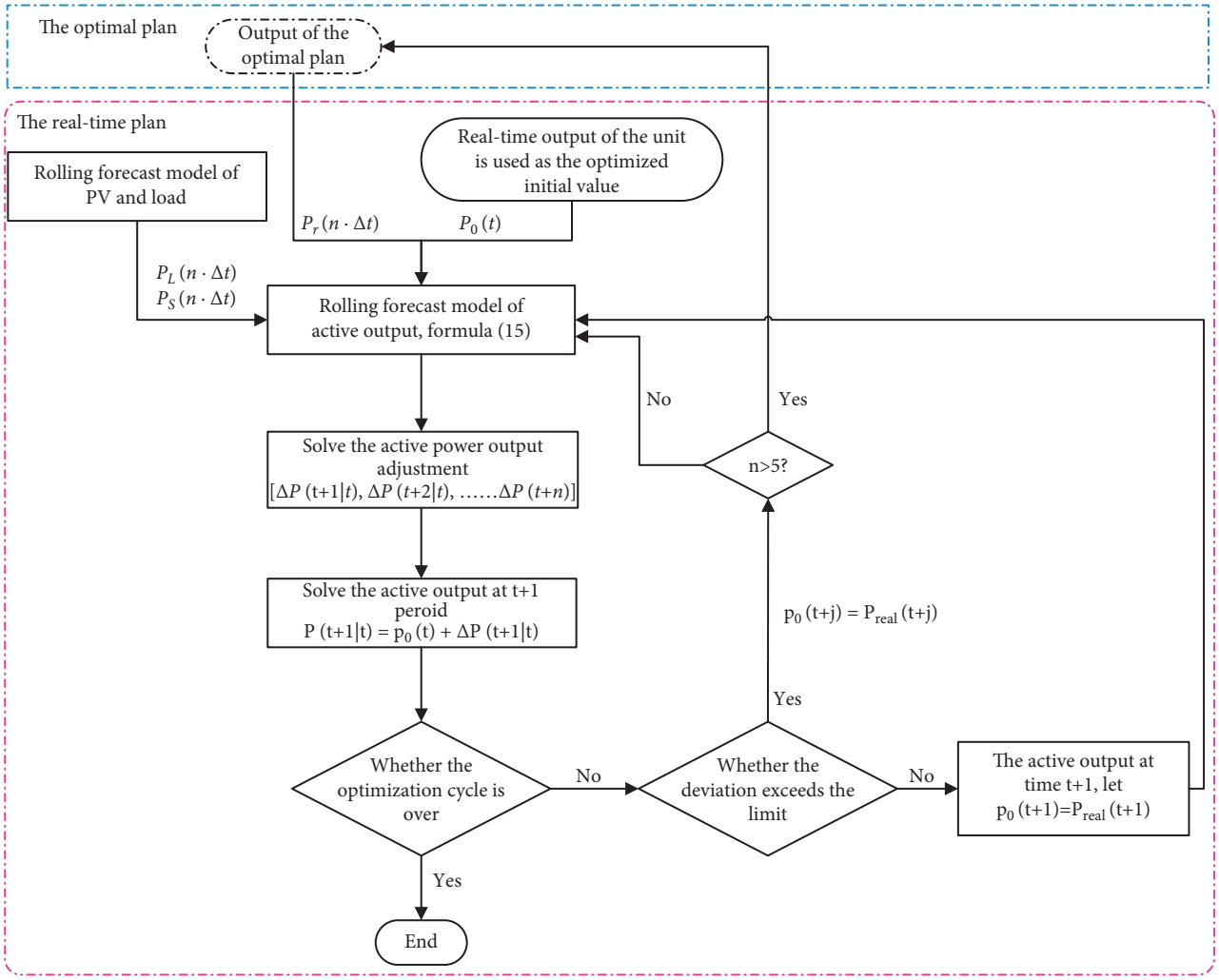

Figure 3: Flowchart of the dynamic optimization process of the active power.

Table 1: Operating parameters of the power stations.

Generation station	Installed capacity (MW)	Number of units	Ability of reservoir capacity adjustment	Upper reservoir capacity (initial reservoir) (10^4 m^3)	Hydraulic head (initial hydraulic head) (m)	Generation flow (m^3)
First level	45	3	Daily regulation	30.1 (15.5)	112.8–134.5 (117.4)	43.32
Second level	60	3	Daily regulation	96.1 (83.6)	125.5–156.5 (140.2)	53.4
Third level CH	36	3	Daily regulation	70 (53)	91–130 (123.3)	33
PS	5	1	Daily regulation	25.6	100	—
PV	50	1	—	—	—	—

was not available. At approximately 6 pm, owing to a significant drop in the PV output, the hydropower units that had been previously stopped were gradually opened to ensure that the load demand could be met.

To reflect the feasibility and effectiveness of the proposed HSC method based on model predictive control, two simulations were performed. In the first simulation, there were no load fluctuations but only PV fluctuations (Case 1), and in the second simulation, there were both load and PV fluctuations (Case 2). Case 1 was used to demonstrate the improvement in the PV generation absorption capacity achieved using the HSC method based on model predictive control. Considering fluctuations in both load and PV generation output, Case 2 was used to reflect the improvement in the safety and stability of the multienergy complementary power generation system after the addition of PV generation by the HSC method. The two cases were simulated for both the traditional open-loop optimization method and the hierarchical optimization scheduling methods.

As shown in the first graph in Figure 5, compared to the traditional open-loop optimization method based on the hour-ahead forecast for optimal scheduling control, the hierarchical open-loop optimization method (compared

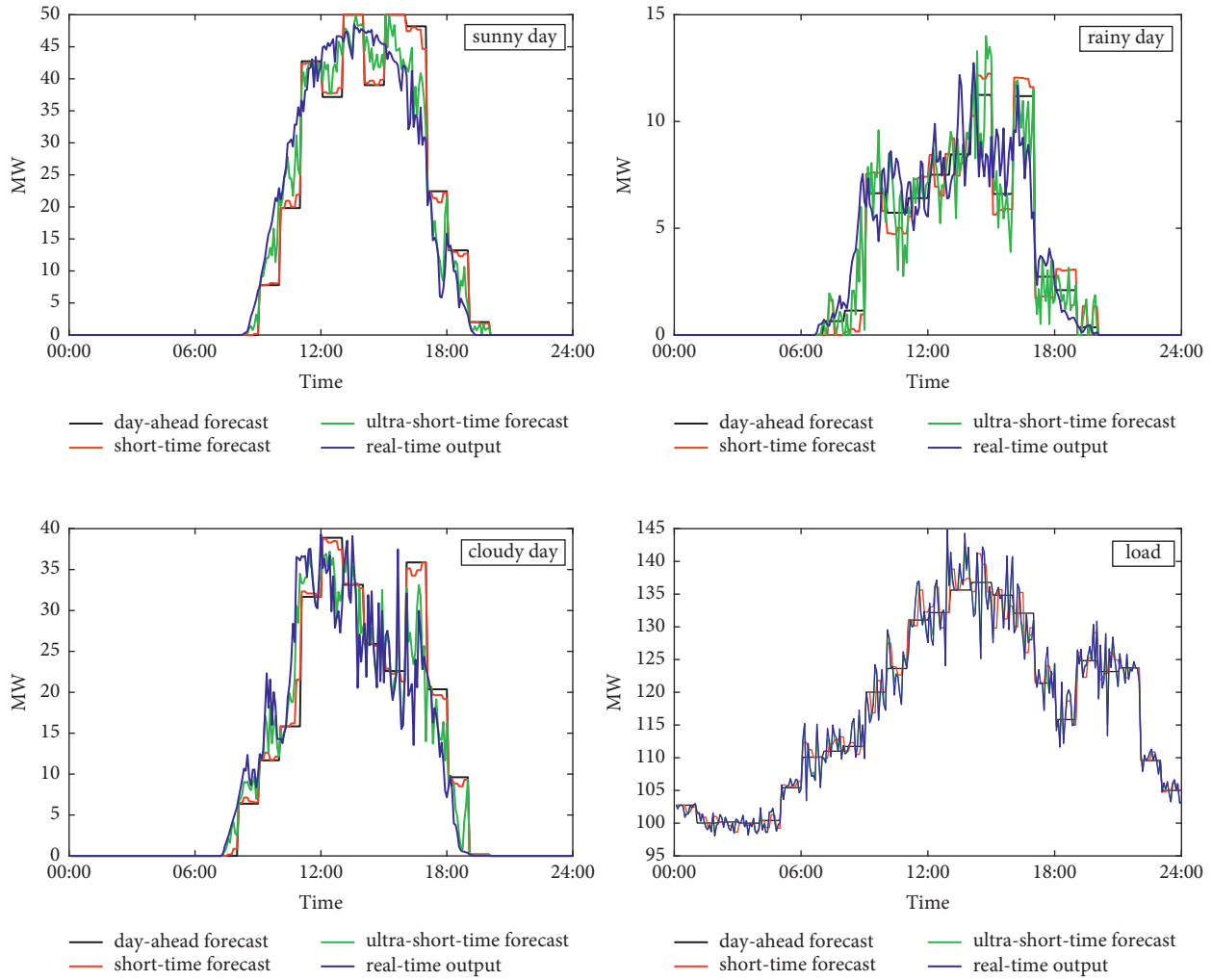

Figure 4: Comparison of the forecasted PV and load data and the real-time output of the analyzed system.

Table 2: Start and stop conditions of all units of the generation stations on a sunny day.

Unit	Time																							
	01:00	02:00	03:00	04:00	05:00	06:00	07:00	08:00	09:00	10:00	11:00	12:00	13:00	14:00	15:00	16:00	17:00	18:00	19:00	20:00	21:00	22:00	23:00	24:00
Output of units of the first-stage power station																								
Unit 1	**1**	**1**	**1**	**1**	**1**	**1**	**1**	**1**	**1**	**1**	**1**	**1**	**1**	**1**	**1**	**1**	**1**	**1**	**1**	**1**	**1**	**1**	**1**	**1**
Unit 2	**1**	**1**	**1**	**1**	**1**	**1**	**1**	**1**	**1**	**1**	**1**	**1**	**1**	**1**	**1**	**1**	**1**	**1**	**1**	**1**	**1**	**1**	**1**	**1**
Unit 3	**1**	**1**	**1**	**1**	**1**	**1**	**1**	**1**	**1**	**1**	**0**	**0**	**0**	**0**	**0**	**0**	**0**	**0**	**1**	**1**	**1**	**1**	**0**	**0**
Output of units of the second-stage power station																								
Unit 1	**1**	**1**	**1**	**1**	**1**	**1**	**1**	**1**	**1**	**1**	**1**	**1**	**1**	**1**	**1**	**1**	**1**	**1**	**1**	**1**	**1**	**1**	**1**	**1**
Unit 2	**1**	**1**	**1**	**1**	**1**	**1**	**1**	**1**	**1**	**1**	**1**	**1**	**1**	**1**	**1**	**1**	**1**	**1**	**1**	**1**	**1**	**1**	**1**	**1**
Unit 3	**1**	**1**	**1**	**1**	**1**	**1**	**1**	**1**	**1**	**1**	**1**	**1**	**0**	**0**	**0**	**0**	**0**	**1**	**1**	**1**	**1**	**1**	**1**	**1**
Output of units of the third-stage power station																								
Unit 1	**1**	**1**	**1**	**1**	**1**	**1**	**1**	**1**	**1**	**1**	**1**	**1**	**1**	**1**	**1**	**1**	**1**	**1**	**1**	**1**	**1**	**1**	**1**	**1**
Unit 2	**1**	**1**	**1**	**1**	**1**	**1**	**1**	**1**	**1**	**1**	**1**	**1**	**1**	**1**	**1**	**1**	**1**	**1**	**1**	**1**	**1**	**1**	**1**	**1**
Unit 3	**1**	**1**	**0**	**0**	**0**	**0**	**0**	**0**	**0**	**0**	**0**	**0**	**0**	**0**	**0**	**0**	**0**	**0**	**1**	**1**	**1**	**1**	**1**	**1**

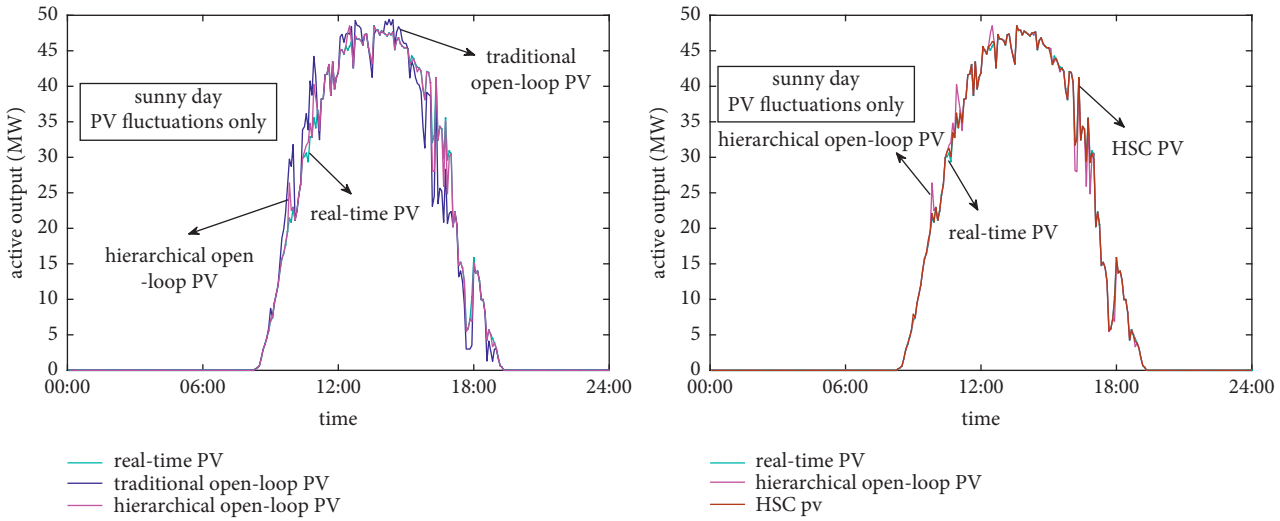

Figure 5: Comparison of PV generation of different methods on a sunny day for Case 1.

with the HSC, this method lacks feedback correction) further refined the time scale and improved the prediction accuracy. The result of the hierarchical open-loop optimization method was significantly better than that of the traditional open-loop optimization method. In addition, Figure 5 shows that the hierarchical scheduling control based on the MPC refined the time scale. The output schedule of the conventional hydropower units was corrected by the introduced feedback, so the consumption of PV generation was closer to the actual PV output. To evaluate the ability of each of the methods to absorb PV generation, the PV follow-up degree and average relative deviation were used as quantitative indicators, and they were, respectively, calculated by

$$\eta_g = 1 - \frac{n_p^d}{n_{p,\text{all}}},$$
$$\eta_e = \frac{\sum_{n=1}^{n=n_p^d} \left| P_{p,n}^d \right|}{n_p^d \overline{P}}. \tag{24}$$

The specific quantitative simulation results are given in Table 3. As shown in Table 3, the proposed HSC method based on the MPC achieved better following degree and average relative deviation than the traditional open-loop optimization and hierarchical optimization methods.

To further analyze the improvement in the operational stability of the complementary generation system achieved by the HSC method, the effectiveness of the HSC method was examined under conditions of load fluctuations and PV output uncertainties, and the simulation analysis results of the traditional open-loop optimization and hierarchical open-loop optimization under the same scenario were compared with those of the HSC method. The evaluation index of the stability of the complementary power generation system was analyzed based on the following parameters:

Load-following degree:

$$\eta_{gL} = 1 - \frac{n_L^d}{n_{L,\text{all}}}. \tag{25}$$

Average load relative deviation:

$$\eta_{eL} = \frac{\sum_{n=1}^{n=n_L^d} \left| P_{L,n}^d \right|}{n_L^d \overline{P_L}} \tag{26}$$

Reliability deviation:

$$\lambda = \frac{P_L^{d,\max} - P_{L,\text{real}}}{\overline{P_L}}. \tag{27}$$

As shown in Figure 6, the traditional open-loop optimization method approached the actual load demand situation, but the hierarchical open-loop optimization more closely followed the short-time fluctuations in the actual load. Further comparing the hierarchical open-loop optimization method and the HSC method showed that the HSC method based on the MPC could adjust the output schedule and thus met the predefined requirements, which was due to the addition of predictive models and feedback correction links. Therefore, the HSC power output could be more suitable for actual load demand compared with that of the hierarchical open-loop optimization method. The cascade hydropower outputs of the three methods are shown in Figure 7, where it can be seen that the cascade hydropower outputs were similar, but there were certain deviations.

The comparison results of the load-following degree, average relative load deviation, and reliability deviation performance metrics of the hierarchical open-loop optimization and HSC methods with the traditional open-loop method are presented in Table 4. Although the improvement in the average relative load deviation was smaller than that in the follow-up and reliability deviation, there was still a significant improvement in the PV power generation consumption when the HSC method was compared with the hierarchical open-loop optimization.

Table 3: PV generation capacity when the load changes are neglected.

Method	Traditional open loop (%)	Hierarchical optimization (%)	HSC (%)
Follow-up degree	63.2	78.9	79.7
Average relative deviation	13.7	6.9	1.9

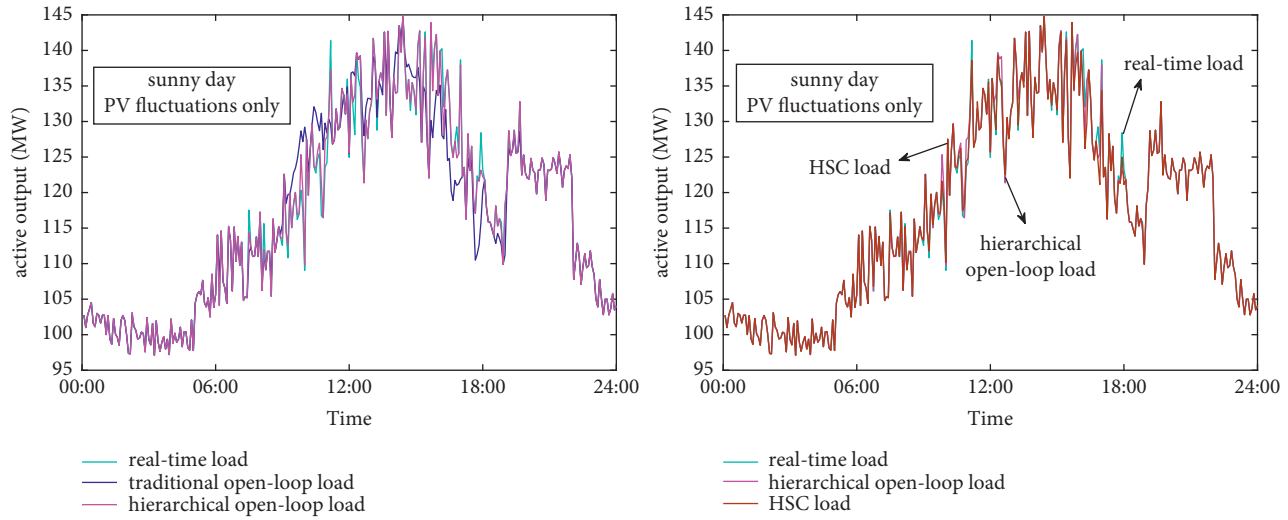

Figure 6: Comparison of the load-following degree of different methods on a sunny day for Case 2.

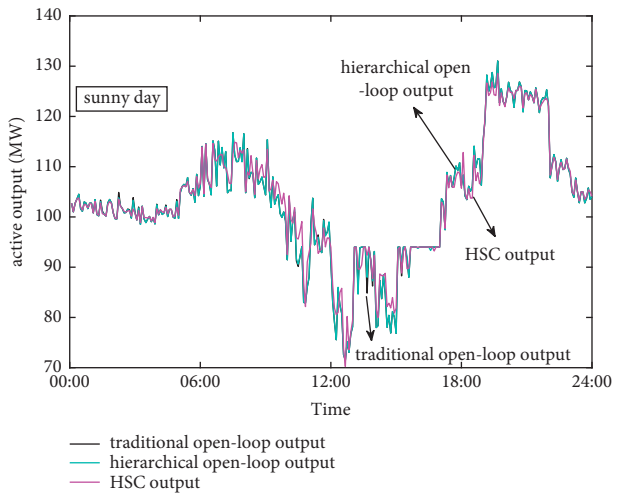

Figure 7: Comparison of total outputs of the cascade power stations under different conditions on a sunny day.

Table 4: Comparison of the load-following degree of different methods.

Method	Traditional open loop (%)	Hierarchical optimization (%)	HSC (%)
Load-following degree	67.1	86.8	87.2
Average relative load deviation	4.5	2.0	1.1
Reliability deviation	17.2	5.0	4.4

5.2. Simulation of PV Generation System on Rainy Days. The start-up and shutdown schedules of the units used in this simulation are given in Table 5, where it can be seen that compared with the start-up and shutdown conditions under sunny weather, the PV generation output under rainy weather was lower. Each unit of the second-level power station was turned on during the day to meet the load demand. Unit 3 of the third-level power station was shut down during certain periods in a day because the load during these periods was reduced.

As shown in Figure 8, on rainy days, compared with the traditional open-loop and hierarchical open-loop optimization methods, the HSC method based on the MPC, which included the refined time scale and the introduction of model predictive control methods, achieved output closer to the actual PV output, so better results could be obtained for PV generation consumption.

As shown in Table 6, the hierarchical open-loop optimization method, after further refinement of the time scale, achieved a significant improvement in the follow-up degree and average relative deviation compared with the traditional open-loop optimization. Although the HSC method did not improve the follow-up degree compared with the hierarchical open-loop optimization method, it achieved a significant improvement in the average relative load deviation, which was because the PV generation output was very low under rainy weather conditions. To meet the load demand, each unit of the hydropower station had at a relatively high-output level. Owing to the influence of operating conditions and other factors, adjustable range of the HSC method was insufficient compared to the normal situation, resulting in a slight improvement in the follow-up degree.

Table 5: Start and stop conditions of all units of the generation stations on a rainy day.

Unit	Time																							
	01:00	02:00	03:00	04:00	05:00	06:00	07:00	08:00	09:00	10:00	11:00	12:00	13:00	14:00	15:00	16:00	17:00	18:00	19:00	20:00	21:00	22:00	23:00	24:00
Output of units of the first-stage power station																								
Unit 1	**1**	**1**	**1**	**1**	**1**	**1**	**1**	**1**	**1**	**1**	**1**	**1**	**1**	**1**	**1**	**1**	**1**	**1**	**1**	**1**	**1**	**1**	**1**	**1**
Unit 2	**1**	**1**	**1**	**1**	**1**	**1**	**1**	**1**	**1**	**1**	**1**	**1**	**1**	**1**	**1**	**1**	**1**	**1**	**1**	**1**	**1**	**1**	**1**	**1**
Unit 3	**1**	**1**	**1**	**1**	**1**	**1**	**1**	**1**	**1**	**1**	**1**	**1**	**1**	**1**	**1**	**1**	**1**	**1**	**1**	**1**	**1**	**1**	**1**	**1**
Output of units of the second-stage power station																								
Unit 1	**1**	**1**	**1**	**1**	**1**	**1**	**1**	**1**	**1**	**1**	**1**	**1**	**1**	**1**	**1**	**1**	**1**	**1**	**1**	**1**	**1**	**1**	**1**	**1**
Unit 2	**1**	**1**	**1**	**1**	**1**	**1**	**1**	**1**	**1**	**1**	**1**	**1**	**1**	**1**	**1**	**1**	**1**	**1**	**1**	**1**	**1**	**1**	**1**	**1**
Unit 3	**1**	**1**	**1**	**1**	**1**	**1**	**1**	**1**	**1**	**1**	**1**	**1**	**1**	**1**	**1**	**1**	**1**	**1**	**1**	**1**	**1**	**1**	**1**	**1**
Output of units of the third-stage power station																								
Unit 1	**1**	**1**	**1**	**1**	**1**	**1**	**1**	**1**	**1**	**1**	**1**	**1**	**1**	**1**	**1**	**1**	**1**	**1**	**1**	**1**	**1**	**1**	**1**	**1**
Unit 2	**1**	**1**	**1**	**1**	**1**	**1**	**1**	**1**	**1**	**1**	**1**	**1**	**1**	**1**	**1**	**1**	**1**	**1**	**1**	**1**	**1**	**1**	**1**	**1**
Unit 3	**1**	**1**	**1**	**0**	**0**	**0**	**0**	**0**	**0**	**1**	**1**	**1**	**1**	**1**	**1**	**1**	**1**	**1**	**1**	**1**	**1**	**1**	**0**	**0**

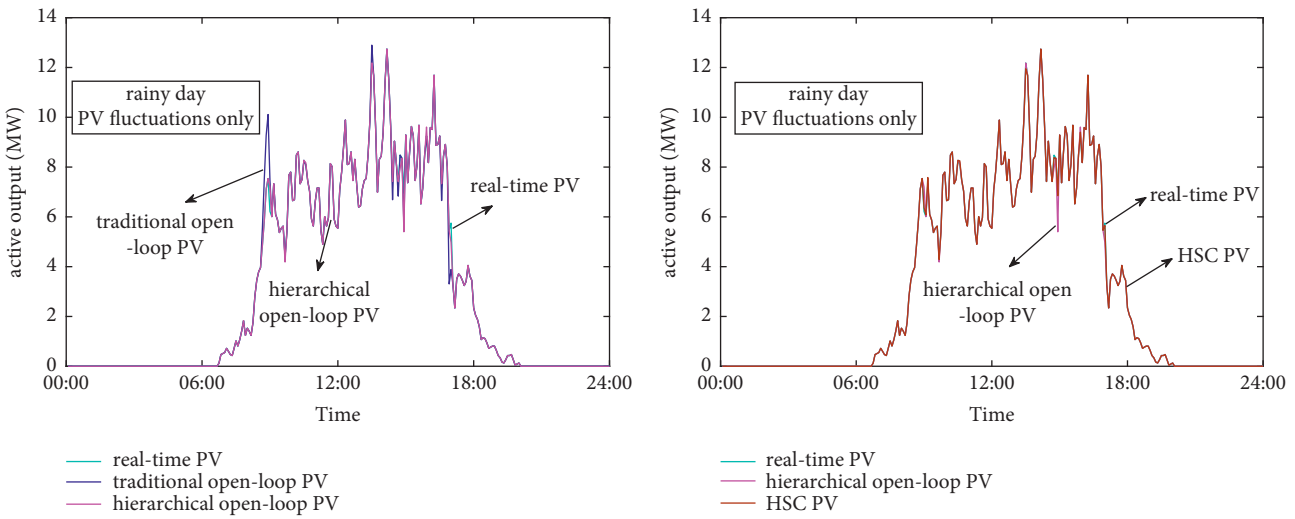

Figure 8: Comparison of PV generation of different methods on a rainy day for Case 1.

Table 6: PV generation capacity under constant load.

Method	Traditional open loop (%)	Hierarchical optimization (%)	HSC (%)
Follow-up degree	87.5	92.5	92.5
Average relative deviation	25.1	11.7	2.8

According to the results presented in Figures 9 and 10 and Table 7, the fluctuation in the PV generation output had little impact on the complementary power generation system. This could be because the PV generation output was not high under rainy weather, and due to the low PV output, even the traditional open-loop optimization can achieve better results. However, considering the load uncertainty, the superposition of the load and PV fluctuations could have a certain influence on the system output. After refining the time scale, the hierarchical open-loop optimization is better than the traditional open-loop optimization in each performance index. Since the HSC method based on the MPC introduced the model predictive control method and added feedback correction link, the output of the cascade

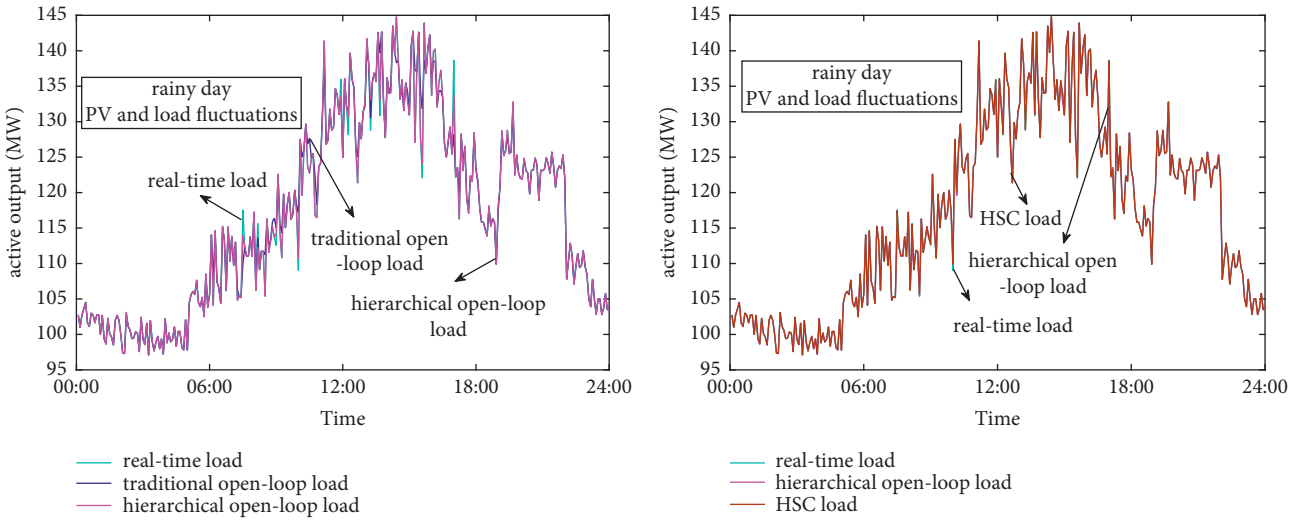

Figure 9: Comparison of the load-following ability of different methods on a rainy day for Case 2.

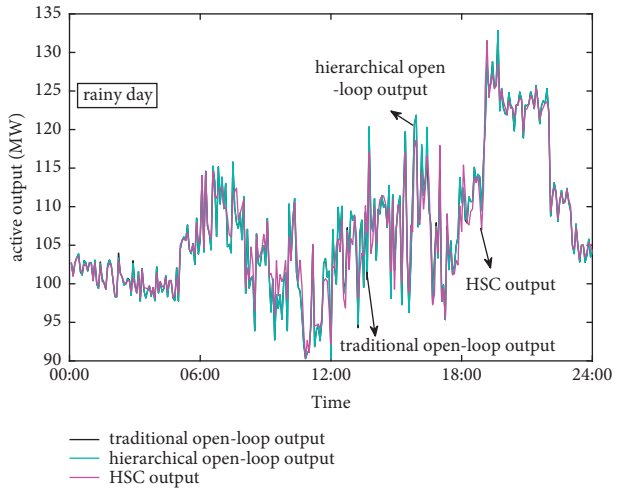

Figure 10: Comparison of total outputs of the cascade power stations under different conditions on a rainy day.

Table 7: Comparison of the load-following degree of different methods.

Method	Traditional open loop (%)	Hierarchical optimization (%)	HSC (%)
Load-following degree	81.9	92.3	92.7
Average relative load deviation	3.9	2.0	1.0
Reliability deviation	9.0	4.2	1.1

hydropower station could handle the superimposed fluctuation energy of the system within the required range, thereby improving the safety and stability of the complementary power generation system.

5.3. Simulation of PV Generation System on Cloudy Days. The start and stop conditions of all cascade hydropower stations under cloudy weather are shown in Table 8, where it can be seen that, to avoid water abandonment, the downtimes of the units in the first and second cascade hydropower stations were in the low-load period. In addition, to ensure unnecessary water abandonment, the shutdown period of the third-level power station's units was during the daytime when there was a certain PV generation output.

Based on the results in Figure 11 and Table 9, owing to the large volatility in the PV generation output under cloudy weather, the traditional open-loop optimization had a weak ability to absorb PV generation output, and although the hierarchical open-loop optimization of the refined time scale could increase the absorption capacity of PV to a certain extent, owing to the capacity limitations of the pumped storage units used to compensate for the rapid fluctuation in PV generation, satisfactory results could not be achieved. In

Table 8: Start and stop conditions of units of the generation stations on a cloudy day.

Unit	Time																							
	01:00	02:00	03:00	04:00	05:00	06:00	07:00	08:00	09:00	10:00	11:00	12:00	13:00	14:00	15:00	16:00	17:00	18:00	19:00	20:00	21:00	22:00	23:00	24:00
Output of units of the first-stage power station																								
Unit 1	**1**	**1**	**1**	**1**	**1**	**1**	**1**	**1**	**1**	**1**	**1**	**1**	**1**	**1**	**1**	**1**	**1**	**1**	**1**	**1**	**1**	**1**	**1**	**1**
Unit 2	**1**	**1**	**1**	**1**	**1**	**1**	**1**	**1**	**1**	**1**	**1**	**1**	**1**	**1**	**1**	**1**	**1**	**1**	**1**	**1**	**1**	**1**	**1**	**1**
Unit 3	**1**	**0**	**0**	**0**	**1**	**1**	**1**	**1**	**1**	**1**	**1**	**1**	**1**	**1**	**1**	**1**	**1**	**1**	**1**	**1**	**1**	**1**	**0**	**0**
Output of units of the second-stage power station																								
Unit 1	1	1	1	1	1	1	1	1	1	1	1	1	1	1	1	1	1	1	1	1	1	1	1	**1**
Unit 2	1	1	1	1	1	1	1	1	1	1	1	1	1	1	1	1	1	1	1	1	1	1	1	**1**
Unit 3	0	1	1	1	1	1	1	1	1	1	1	1	1	1	1	1	1	1	1	1	1	1	0	**0**
Output of units of the third-stage power station																								
Unit 1	**1**	**1**	**1**	**1**	**1**	**1**	**1**	**1**	**1**	**1**	**1**	**1**	**1**	**1**	**1**	**1**	**1**	**1**	**1**	**1**	**1**	**1**	**1**	**1**
Unit 2	**1**	**1**	**1**	**1**	**1**	**1**	**1**	**1**	**1**	**1**	**1**	**1**	**1**	**1**	**1**	**1**	**1**	**1**	**1**	**1**	**1**	**1**	**1**	**1**
Unit 3	**1**	**1**	**1**	**1**	**0**	**0**	**0**	**0**	**0**	**0**	**0**	**0**	**0**	**0**	**0**	**0**	**0**	**0**	**0**	**1**	**1**	**1**	**1**	**0**

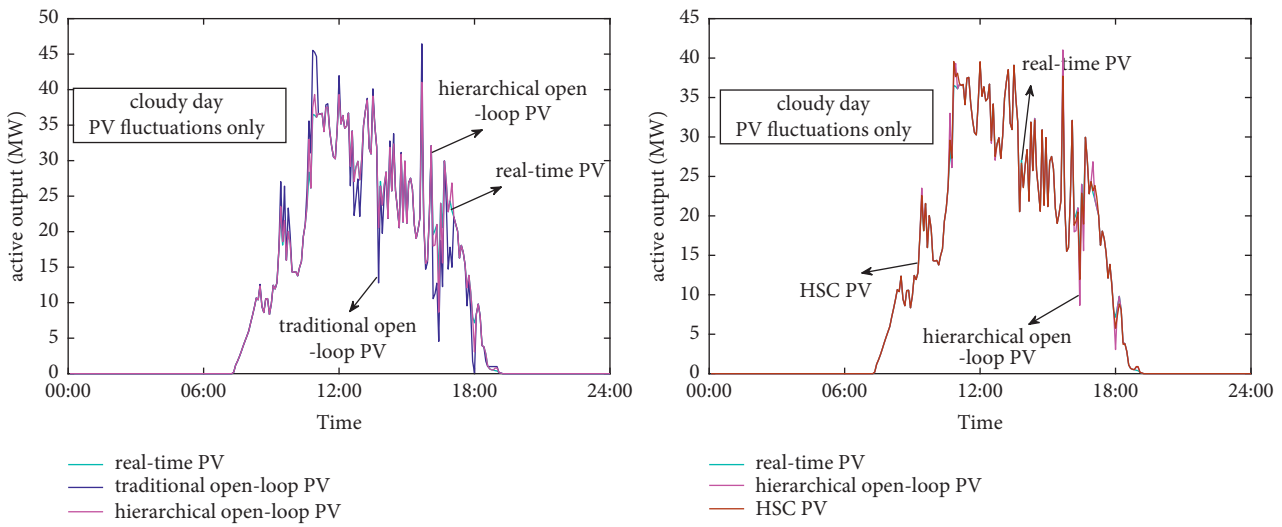

Figure 11: Comparison of PV generation of different methods on a cloudy day for Case 1.

Table 9: PV generation capacity under a constant load.

Method	Traditional open loop (%)	Hierarchical optimization (%)	HSC (%)
Follow-up degree	58.7	76.2	88.1
Average relative deviation	18.8	12.3	3.6

contrast, the HSC method based on the MPC not only refined the time scale but also fed back and corrected the output of the cascade hydropower units according to the actual operating conditions. Also, it showed a more sufficient compensation ability under larger fluctuations in the PV generation output and further improved the ability of the power generation system to respond to changes in the PV generation, thereby improving the ability of the complementary power generation system to absorb PV generation.

According to the results in Figures 12 and 13 and Table 10, the HSC method based on MPC did not achieve significant improvement in the load-following degree compared with the

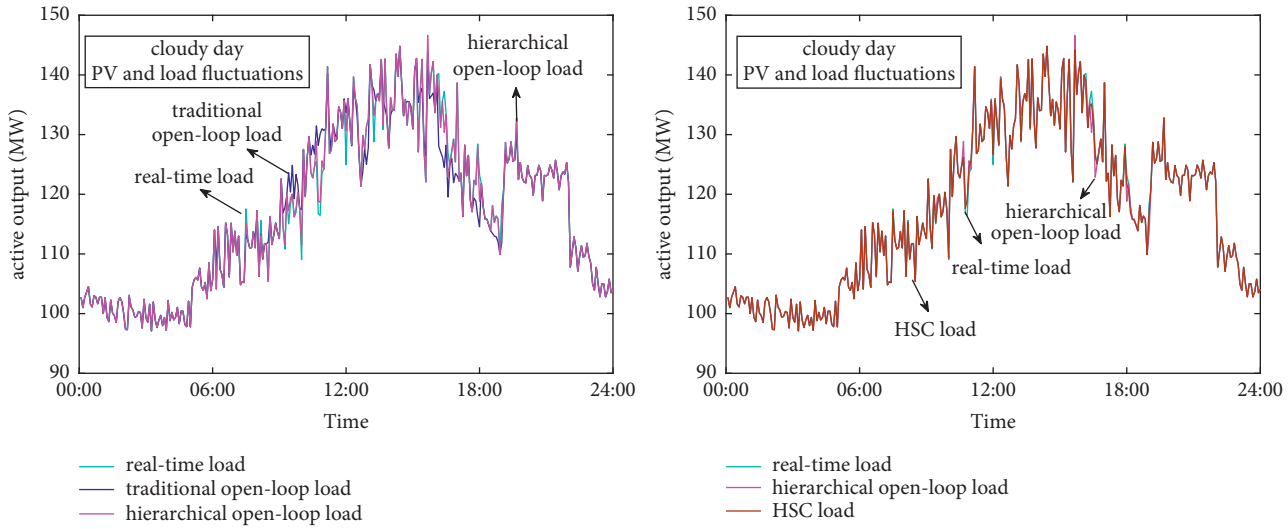

Figure 12: Comparison of the load-following ability of different methods on a cloudy day for Case 2.

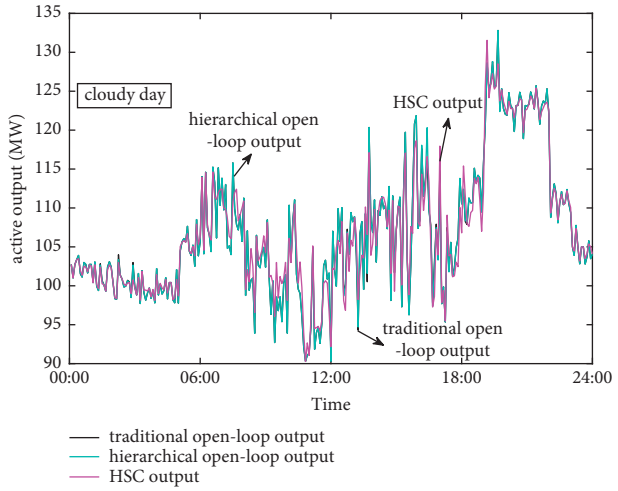

Figure 13: Comparison of total outputs of the cascade power stations under different conditions on a cloudy day.

Table 10: Comparison of the load-following degree of different methods.

Method	Traditional open loop (%)	Hierarchical optimization (%)	HSC (%)
Load-following degree	74.3	86.1	88.9
Average relative load deviation	2.6	1.8	0.8
Reliability deviation	13.3	5.9	2.2

hierarchical optimization method, which could be due to the addition of predictive models, rolling optimization, and feedback correction links. The HSC method had a more flexible adjustment ability for superimposed fluctuations in the load and PV, so its average relative load deviation and reliability deviation were greatly improved compared with the hierarchical open-loop optimization method.

5.4. Economic Comparison. Considering the electricity selling price of 0.4 yuan, the economic benefits of different methods under three typical scenarios of sunny, cloudy, and rainy weather are shown in Table 11. As shown in Table 11, compared to the traditional open-loop optimized and hierarchical optimization methods, the HSC method that controlled the active power output of the controllable generation units in the CH-PV-PS system through coordinated dispatch achieved significant economic benefits in both cases, under the load fluctuations and without load fluctuations of 23.7/1.3/3.1 thousands of yuan and 12.3/1.2/1.6 thousands of yuan and 17.8/3.8/3.7 thousands of yuan and 0.2/0.3/0.4 thousands of yuan, respectively.

Table 11: Comparison of the comprehensive benefits of the system of the three methods on a sunny day.

Method	Constant load (thousands of yuan)	Variable load (thousands of yuan)
Traditional open loop	1171.5/1314.8/1229.2	1331.5/1344.9/1345.2
Hierarchical optimization	1182.9/1314.9/1230.7	1349.1/1348.4/1348.5
HSC	1195.2/1316.1/1232.3	1349.3/1348.7/1348.9

6. Conclusion

In this paper, an HSC method for the CH-PV-PS generation system was proposed to reduce the impact of PV output uncertainty, which layered optimal scheduling control to refine the time scale. Based on this, MPC method is introduced, which utilizes the fast response capability of CHS and PS to cope with the rapid changes of PV and load, ensuring the safe and stable operation of CH-PV-PS generation system while improving the PV consumption capacity. The simulation results demonstrate that the proposed HSC method can effectively improve the PV consumption capacity and system operation stability of the CH-PV-PS generation system while ensuring the maximum comprehensive economic benefits. This HSC method provides an effective solution to the current problem of dissipation of a large number of new energy sources with uncertain power output to the grid.

Nomenclature

N: Length of the optimized time period
$P_{ij,T}$: Output of the jth unit of the ith CH station at time T
$P_{s,T}$: PV output at time T
$P_{f,T}$: PS's power generation and pumping at time T
$P_{p,T}$: PS's pumping at time T, respectively
C_T: Electricity price at time T
$C_{q,T}$: Penalty price for abandoning water at time T
$P_{w,T}$: Amount of abandoned water at time T
C_{sT}: Unit starting and stop cost at time T
$\boldsymbol{U}_T$: Vector combinations of the start states of the units
$\boldsymbol{D}_T$: Vector combinations of the stop states of the units
$P_{L,T}$: Load demand at time T
$V_{i,T}$: Storage capacity of the ith power station at time T
$I_{i,T}$: Inflow of the ith power station at time T
$d_{i,T}$: Discarded water flow of the ith power station at time T
$Q_{i,T}$: Power generation flow of the ith power station at time T
$Q_{i,max}$: Upper limits of the power generation flow of the ith power station
$Q_{i,min}$: Lower limits of the power generation flow of the ith power station, respectively
$V_{i,max}$: Upper limits of the storage capacity of the ith power station
$V_{i,min}$: Lower limits of the storage capacity of the ith power station
$H_{i,max}$: Upper limits of the water head of the ith stage power station
$H_{i,min}$: Lower limits of the water head of the ith stage power station
$P_{\max}$: Upper limits of the unit output
$P_{\min}$: Lower limits of the unit output
$P_{ij,T}^{\mathrm{up}}$: Upper limits of the j unit restriction zone of the ith-level hydropower station
$P_{ij,T}^{\mathrm{do}}$: Lower limits of the j unit restriction zone of the ith-level hydropower station
T_{ijon}: Minimum unit online time
T_{ijoff}: Minimum off-grid time
P_T: Output schedule at time T
$\Delta \mathrm{P}^{\mathrm{up}}$: Limit of the lift range of the unit during one period
$P(t+\Delta t|t)$: Predicted active output value of controllable power generation units in the period $(t+\Delta t)$ obtained at time t
$P_0(t)$: Current output value at time t, the initial value
$\Delta p(t+k|t)$: Predicted increase in the active power output at the next time step $(t+k)$ as obtained at time t
n: Prediction step of the active power output
P_r: Reference output derived from the result of the static optimization layer and the ultra-short-term forecast information on the load and PV
P_t: Output at time t
$\Delta P^{m,\mathrm{up}}$: Upper limit of the lifting amplitude
γ: Upper limit of the unit action dead zone, and when the distributed load is less than this value, the unit will not act
η_g: Follow-up degree of PV generation
n_p^d: Number of periods when PV generation was not completely absorbed
$n_{p,all}$: Number of total output periods of PV generation
η_e: Average relative deviation in PV generation consumption
$P_{p,n}^d$: Remaining PV that had not been consumed
$\overline{P}$: Average value of PV generation
η_{gL}: Load-following degree
n_L^d: Number of time periods when the load is not fully followed
$n_{L,all}$: Number of time periods
η_{eL}: Average relative load deviation
$P_{L,n}^d$: Difference between the scheduled output and the actual output
$\overline{P}_L$: Average load demand in the optimized time domain
λ: Reliable coefficient in the optimized time domain

$P_L^{d,\max}$: Maximum output deviation in the optimized time domain
P_{real}: Actual output value of the system.

Data Availability

The data that support the findings of this study are available from the corresponding author upon reasonable request.

Conflicts of Interest

The authors have no conflicts of interest to disclose regarding the publication of this paper.

Acknowledgments

This work was supported by the National Key Research and Development Program (Grant no. 2018YFB0905200) and by Sichuan Science and Technology Program (Grant nos. 2021YFG0204, 2022NSFSC0025, 2022YFS0538, and 2022YFG0117).

References

[1] B. François, B. Hingray, D. Raynaud, M. Borga, and J. D. Creutin, "Increasing climate-related-energy penetration by integrating run-of-the river hydropower to wind/solar mix," *Renewable Energy*, vol. 87, pp. 686–696, 2016.

[2] L. Che, X. Zhang, M. Shahidehpour, A. Alabdulwahab, and A. Abusorrah, "Optimal interconnection planning of community microgrids with renewable energy sources," *IEEE Transactions on Smart Grid*, vol. 8, no. 3, pp. 1054–1063, 2017.

[3] H. Zhang, W. Hu, R. Yu, and M. Tang, "Coordinated optimal short-term operation of hydro-wind-solar integrated systems," *Energy Procedia*, vol. 158, pp. 6260–6265, 2019.

[4] W. Hu, H. Zhang, Y. Dong, Y. Wang, L. Dong, and M. Xiao, "Short-term optimal operation of hydro-wind-solar hybrid system with improved generative adversarial networks," *Applied Energy*, vol. 250, pp. 389–403, 2019.

[5] I. Kougias, S. Szabó, F. Monforti-Ferrario, T. Huld, and K. Bódis, "A methodology for optimization of the complementarity between small-hydropower plants and solar PV systems," *Renewable Energy*, vol. 87, pp. 1023–1030, 2016.

[6] H. Li, P. Liu, S. Guo, B. Ming, L. Cheng, and Z. Yang, "Long-term complementary operation of a large-scale hydro-photovoltaic hybrid power plant using explicit stochastic optimization," *Applied Energy*, vol. 238, pp. 863–875, 2019.

[7] F. Wang, Y. Xie, and J. Xu, "Reliable-economical equilibrium based short-term scheduling towards hybrid hydro-photovoltaic generation systems: case study from China," *Applied Energy*, vol. 253, Article ID 113559, 2019.

[8] Y. An, W. Fang, B. Ming, and Q. Huang, "Theories and methodology of complementary hydro/photovoltaic operation: applications to short-term scheduling," *Journal of Renewable and Sustainable Energy*, vol. 7, no. 6, Article ID 063133, 2015.

[9] F.-F. Li and J. Qiu, "Multi-objective optimization for integrated hydro-photovoltaic power system," *Applied Energy*, vol. 167, pp. 377–384, 2016.

[10] L. Liu, Q. Sun, Y. Wang, Y. Liu, and R. Wennersten, "Research on short-term optimization for integrated hydro-PV power system based on genetic algorithm," *Energy Procedia*, vol. 152, pp. 1097–1102, 2018.

[11] M. Zhang, T. Xie, C. Zhang, D. Chen, C. Mao, and C. Shen, "Dynamic model and impact on power quality of large hydro-photovoltaic power complementary plant," *International Journal of Energy Research*, vol. 43, no. 9, pp. 4436–4448, 2019.

[12] B. Ming, P. Liu, S. Guo, X. Zhang, M. Feng, and X. Wang, "Optimizing utility-scale photovoltaic power generation for integration into a hydropower reservoir by incorporating long- and short-term operational decisions," *Applied Energy*, vol. 204, pp. 432–445, 2017.

[13] A. H. J. Hounnou, F. Dubas, and F.-X. Fifatin, "Multi-objective optimization of run-of-river small hydro-PV hybrid power systems," *IEEE AFRICON*, vol. 11, no. 5, p. 7, 2019.

[14] B. François, M. Borga, J. D. Creutin, B. Hingray, D. Raynaud, and J. F. Sauterleute, "Complementarity between solar and hydro power: sensitivity study to climate characteristics in northern Italy," *Renewable Energy*, vol. 86, pp. 543–553, 2016.

[15] A. Beluco, P. K. de Souza, and A. Krenzinger, "A dimensionless index evaluating the time complementarity between solar and hydraulic energies," *Renewable Energy*, vol. 33, no. 10, pp. 2157–2165, 2008.

[16] M. Javier, P. Inigo-da-la, G. Miguel, and M. Luis, "Control strategies to smooth short-term power fluctuations in large photovoltaic schedulets using battery storage systems," *Energies*, vol. 7, pp. 6593–6619, 2014.

[17] C. Su, C. Cheng, P. Wang, J. Shen, and X. Wu, "Optimization model for long-distance integrated transmission of wind farms and pumped-storage hydropower plants," *Applied Energy*, vol. 242, pp. 285–293, 2019.

[18] L. Chen, J. Wang, Z. Sun, T. Huang, and F. Wu, "Smoothing photovoltaic power fluctuations for cascade hydro-PV-pumped storage generation system based on a fuzzy CEEMDAN," *IEEE Access*, vol. 7, no. 1, pp. 172718–172727, 2019.

[19] F. Wu, J. Wang, Z. Sun, T. Wang, L. Chen, and X. Han, "An optimal wavelet packets basis method for cascade hydro-PV-pumped storage generation systems to smooth photovoltaic power fluctuations," *Energies*, vol. 12, no. 24, p. 4642, 2019.

[20] W. X. Jiang, J. C. Liu, X. Y. Han et al., "Reserve optimization for offline multi-energy complementary generation system in short time scale," *Power System Technology*, vol. 44, no. 07, pp. 2492–2502, 2020.

[21] T. Li, W. Hu, X. Xu et al., "Optimized operation of hybrid system integrated with MHP, PV and PHS considering generation/load similarity," *IEEE Access*, vol. 7, pp. 107793–107804, 2019.

[22] J. Liu, J. Li, Y. Xiang, and S. Hu, "Optimal sizing of hydro-PV-pumped storage integrated generation system considering uncertainty of PV, load and price," *Energies*, vol. 12, no. 15, p. 3001, 2019.

[23] X. Huang, J. Wang, T. Huang, H. Peng, X. Song, and S. Cheng, "An optimal operation method of cascade hydro-PV-pumped storage generation system based on multi-objective stochastic numerical P systems," *Journal of Renewable and Sustainable Energy*, vol. 13, no. 1, Article ID 016301, 2021.

[24] X. Y. Han, L. J. Ding, G. Chen, J. Y. Liu, and J. Lin, "Key technologies and research prospects for cascaded hydro-photovoltaic-pumped storage hybrid power generation system," *Transactions of China Electrotechnical Society*, vol. 35, no. 13, pp. 2711–2722, 2020.

[25] X. Liu, M. Ding, Y. Zhang, and N. Xu, "Dynamic economic dispatch for microgrids," *Proceedings of the CSEE*, vol. 31, no. 31, pp. 77–84, 2011.

[26] W. Huang, S. Liu, Y. Yi, W. U. Zhaolong, and Y. Zhang, "Multi-time-scale slack optimal control in distribution

network based on voltage optimization for point of common coupling of PV," *Automation of Electric Power Systems*, vol. 43, no. 03, pp. 92–100, 2019.

[27] S. Liu, A. I. Qian, J. Zheng, and R. Wu, "Bi-Level coordination mechanism and operation strategy of multi-time scale multiple virtual power plants," *Proceedings of the CSEE*, vol. 38, no. 03, pp. 753–761, 2018.

[28] H. Q. Yang, Y. C. Pu, Y. B. Qiu, Q. Li, and W. R. Chen, "Multi-time scale integration of robust optimization with MPC for islanded hydrogen based microgrid," in *Proceedings of the IEEE Sustainable Power and Energy Conference (iSPEC)*, pp. 1163–1168, Beijing, China, November 2019.